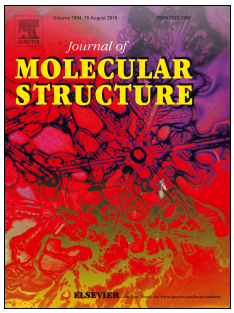

Straightforward synthesis, spectroscopic characterizations and comprehensive DFT calculations of novel 1-ester 4-sulfonamide-1,2,3-triazole scaffolds

Maryam Alizadeh, Zohreh Mirjafary, Hamid Saeidian

PII: S0022-2860(19)31514-5

DOI: https://doi.org/10.1016/j.molstruc.2019.127405

Reference: MOLSTR 127405

To appear in: *Journal of Molecular Structure*

Received Date: 4 June 2019

Revised Date: 24 October 2019

Accepted Date: 11 November 2019

Please cite this article as: M. Alizadeh, Z. Mirjafary, H. Saeidian, Straightforward synthesis, spectroscopic characterizations and comprehensive DFT calculations of novel 1-ester 4-sulfonamide-1,2,3-triazole scaffolds, *Journal of Molecular Structure* (2019), doi: https://doi.org/10.1016/j.molstruc.2019.127405.

Straightforward synthesis, spectroscopic characterizations and comprehensive DFT calculations of novel 1-ester 4-sulfonamide-1,2,3-triazole scaffolds

Maryam Alizadeh, Zohreh Mirjafary, Hamid Saeidian

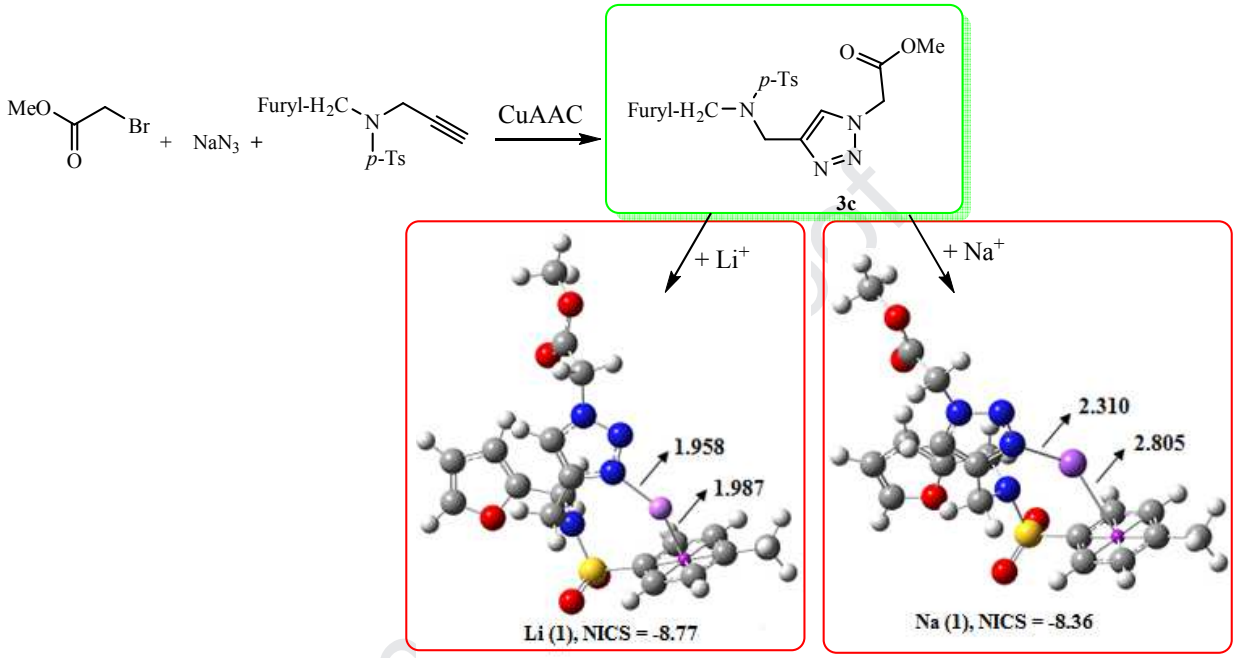

Straightforward synthesis, spectroscopic characterizations and comprehensive DFT calculations of novel 1-ester 4-sulfonamide-1,2,3-triazole scaffolds

Maryam Alizadeh [a], Zohreh Mirjafary [a, *], Hamid Saeidian [b]

[a] Department of Chemistry, Tehran Science and Research Branch, Islamic Azad University, Tehran, Iran

[b] Department of Science, Payame Noor University (PNU), PO Box: 19395-4697, Tehran, Iran

Abstract: For the first time, an efficient click azide–alkyne [3 + 2] cycloaddition reaction for synthesis of new 1-ester 4-sulfonamide-1,2,3-triazole derivatives was developed *via* a three-component reaction of *N*-propargylsulfonamides, sodium azide, and α-haloesters in a one pot method. The mild reaction conditions, avoiding the isolation of hazardous organic azides, good yields (65-78%), and commercially available and inexpensive starting materials are advantages of this cycloaddition reaction for synthesis of fine chemicals. The all desired products were characterized by FT-IR, ^{1}H and ^{13}C NMR spectroscopy. The HOMO-LUMO analysis (electrophilicity index), vibrational frequencies (FT-IR), ^{1}H and ^{13}C chemical shift values and Li^{+} and Na^{+} ion affinities of a desired product have been also calculated by density functional theory (DFT). Lithium ion affinity of the product was determined as 80.78 kJ/mol higher than its sodium ion affinity. The NICS index was used to confirm of the cation π interaction in complex of the synthesized product with Li^{+} and Na^{+} ions.

Keywords: CuAAC reaction; 1,2,3-triazole; *N*-propargylsulfonamide; α-haloester; DFT calculations; cation π interaction.

1. Introduction

1,2,3-Triazoles are important heterocycles, because of their pharmaceuticals and biological activities such as anticancer, antiviral, antibacterials, anticonvulsant, antifungal, HIV protease inhibitors, *etc* [1-6]. Design and preparation of novel 1,4-disubstituted 1,2,3-triazole derivatives are of great importance in organic and medicinal chemistry. The ‘‘click” chemistry protocol,

developed by Sharpless and Meldal, was utilized for regioselective synthesis of 1,4-disubstituted 1,2,3-triazole [7-10]. In this protocol a reactant bearing an azide motif reacts with a terminal alkyne *via* a concerted [3 + 2] cycloaddition of [4πs + 2πs] type in a thermally allowed copper (I)-calalyzed azide alkyne cycloaddition (CuAAC) in the presence of Cu (I) as a catalyst [11-17].

A lot of scientific reports describing the synthetic potencies of the CuAAC reaction have been published. However, there is no example in which this robust method is applied for synthesis of triazole scaffolds containing sulfonamide and ester groups. The ester and sulfonamide groups are key motifs in chemistry and biology [18-20]. Organic molecules that contain triazole, sulfonamide and carbonyl subunits possess various interesting biological activities, such as antiaromatase, carbonic anhydrase isozymes inhibitors, potassium channel activators, antiviral agent and thrombin inhibitors [21–29]. Some examples of biological active triazoles bearing sulfonamide and carbonyl group are shown in Scheme 1.

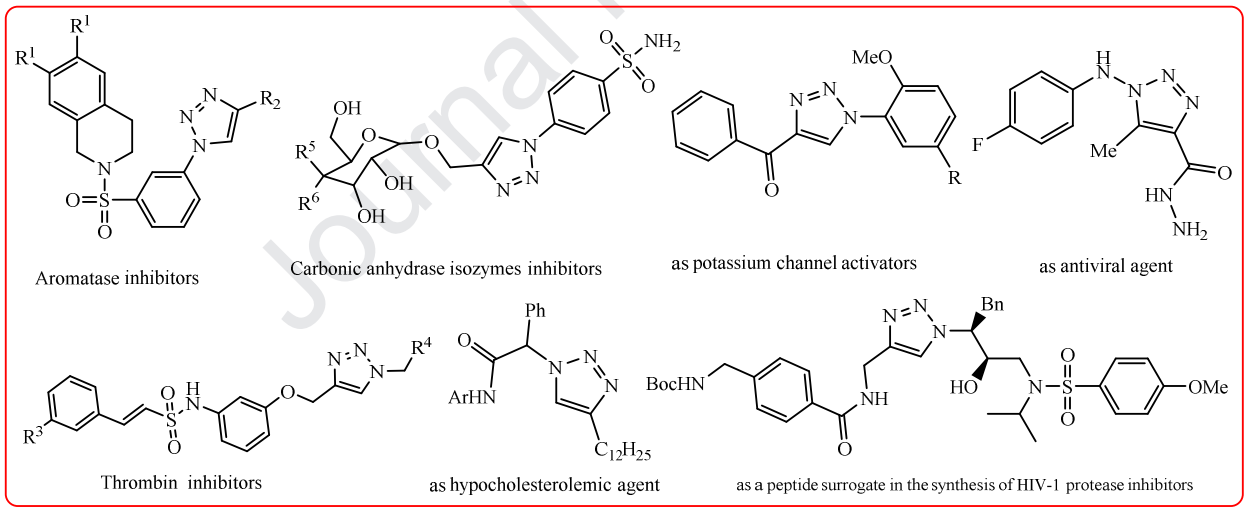

Scheme 1. Some biologically active 1,2,3-triazole scaffolds containing sulfonamide and carbonyl groups.

Recently, we devised highly efficient copper-catalyzed click reaction for synthesis of different type of triazole derivatives, in which a terminal alkyne such as *N*-propargylsulfonamides and bis-(*N*-propargyl) benzodiazepines react with a wide range of alkyl halides and epoxide derivatives in the presence of different sources of copper (I) [30-35]. In the context of our general interest in the

synthesis of heterocycle compounds and following our research on triazole chemistry, for the first time we propose an efficient synthesis for a new series of 1-ester 4-sulfonamide-1,2,3-triazole scaffolds *via* the CuAAC reaction in the presence of CuI as a catalyst (Scheme 2). The structural assignment of the desired products was based on ^{1}H and ^{13}C NMR and FT-IR spectral data.

To make a reasonable assignment of vibrational bands and chemical shifts, density functional theory (DFT) geometry optimization and molecular orbital calculations were performed on the structure of **3c**. 1-Ester 4-sulfonamide-1,2,3-triazole derivatives can be considered as ligand for metal ions, giving a variety of complexes. The Li^{+} and Na^{+} ion affinities of **3c** have been also studied by DFT calculations to find the applicability of these synthesized products for complexation with metal ions.

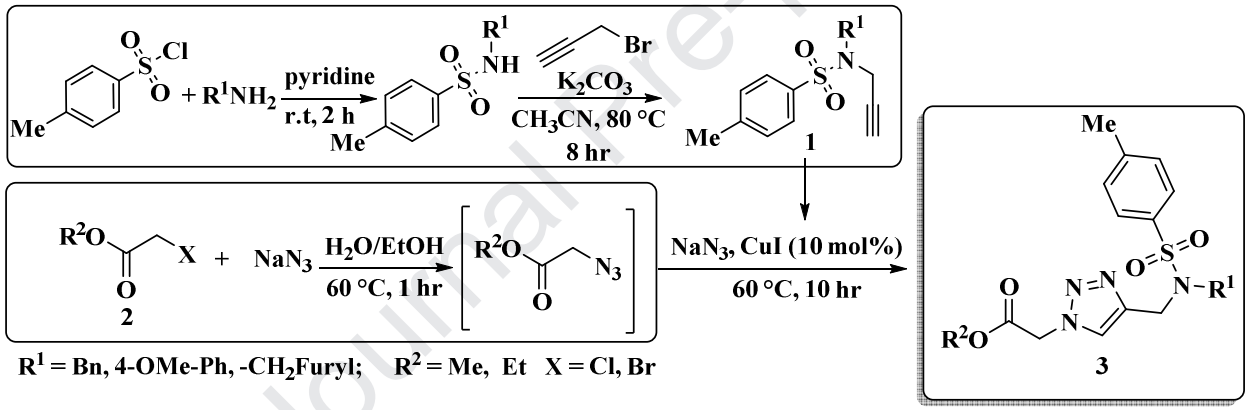

Scheme 2. The efficient method for synthesis of novel 1-ester 4- sulfonamide-1,2,3-triazole scaffolds **3** by the click reaction.

2. Experimental

2. 1. General information

All the chemicals required for the synthesis of 1,2,3-triazoles **3** were purchased from Sigma-Aldrich (St. Louis, MO, USA), Fluka (Neu-Ulm, Germany) and Merck (Darmstadt, Germany) companies and were used as received. The all synthesized compounds gave satisfactory spectroscopic data. A Bruker (DRX-400 Avance) NMR was used to record the ^{1}H and ^{13}C NMR spectra in DMSO at room temperature. FT-IR spectra were taken by a Nicolet spectrometer

(Magna 550), using KBr pellets. All the reactions are monitored by thin layer chromatography (TLC) carried out on silica gel with UV light and iodine, as detecting agents.

2. 2. Computational details

All geometry optimizations and frequency calculations of the desired product **3c** were carried out using the Gaussian 09 software [36]. Density functional theory with the Becke three parameters hybrid functional (DFT-B3LYP/6-31G(d)) calculations were performed for all atoms of **3c**. Vibrational frequencies were calculated at the same level to ensure that each stationary point was a true minimum. After geometry optimization and frequency calculations, zero-point energies (ZPEs) and thermal corrections are obtained at 298 K.

2. 3. General synthesis process for 1,2,3-triazole derivatives 3

α-Haloesters **2** (1 mmol) was dissolved into EtOH/H_2O (1:1, 5 mL). After dissolving, sodium azide (1.2 mmol) was added, and the solution was stirred at room temperature for 1 h then CuI (10% mmol) and *N*-propargylsulfonamide **1** (1 mmol) were added, and the resulted mixture was stirred at 60 ºC until the reaction was over by TLC monitoring. After completion of the reaction, 10 mL of water was added and the mixture was extracted with ethyl acetate. The organic layers were dried over anhydrous sodium sulfate, filtrated and evaporated under vacuum to provide the crude product which was purified by flash column chromatography (silica gel) using ethyl acetate/hexane (1:1) to obtain the desired product **3.**

2.4. Spectral data of the 1-ester 4-sulfonamide-1,2,3-triazole 3

3a: ^{1}HNMR (400 MHz, DMSO): δ = 1.23 (t, *J* = 7.2 Hz, 3H), 2.40 (s, 3H), 4.17 (q, *J* = 7.2 Hz, 2H), 4.36 (s, 2H), 4.39 (s, 2H), 5.33 (s, 2H), 7.23-7.35 (m, 5H), 7.38 (d, *J* = 8.0 Hz, 2H), 7.73 (d, *J* = 8.0 Hz, 2H), 7.87 (s, 1H); ^{13}CNMR (100 MHz, DMSO): δ = 14.42, 21.45, 31.12, 41.93, 50.72, 61.95, 126.08, 127.56, 128.01, 128.69, 128.87, 130.19, 136.60, 136.97, 142.37, 143.68, 167.53 ppm; FT-IR (KBr) : 3138, 2951,1755, 1599, 1447, 1336, 1222, 1157 cm^{-1}. **3b**. ^{1}HNMR (400 MHz, DMSO): δ = 2.39 (s, 3H), 3.73 (s, 3H), 4.37 (s, 2H), 4.39 (s, 2H), 5.36 (s, 2H), 7.27-7.35 (m, 5H),

7.38 (d, *J* = 8.0 Hz, 2H), 7.72 (d, *J* = 8.0 Hz, 2H), 7.88 (s, 1H); ^{13}CNMR (100 MHz, DMSO): δ = 21.45, 41.96, 49.62, 50.61, 52.97, 126.08, 127.56, 128.01, 128.69, 128.87, 130.20, 135.97, 136.60, 142.40, 143.71, 168.03 ppm; FT-IR (KBr) : 3137, 1755, 1599, 1447, 1336, 1222, 1157 cm^{-1}. **3c**: ^{1}HNMR (400 MHz, DMSO): δ = 2.39 (s, 3H), 3.73 (s, 3H), 4.40 (m, 4H), 5.39 (s, 2H), 6.28 (m, 1H), 6.35-6.36 (m, 1H), 7.35 (d, *J* = 8.0 Hz, 2H), 7.53 (m, 1H), 7.69 (d, *J* = 8.0 Hz, 2H), 7.95 (s, 1H); ^{13}CNMR (100 MHz, DMSO): δ = 21.44, 42.15, 43.66, 50.66, 52.98, 110.30, 110.94, 125.87, 127.52, 130.09, 136.79, 142.75, 143.49, 143.66, 149.51, 168.10 ppm; FT-IR (KBr) : 3330, 1750, 1508, 1468, 1417, 1371, 1185, 1026 cm^{-1}. **3d**: ^{1}HNMR (400 MHz, DMSO): δ = 2.41 (s, 3H), 3.69 (s, 3H), 3.72 (s, 3H), 4.87 (s, 2H), 5.37 (s, 2H), 6.84 (d, *J* = 8.8 Hz, 2H), 6.96 (d, *J* = 8.8 Hz, 2H), 7.40 (d, *J* = 8.0 Hz, 2H), 7.55 (d, *J* = 8.0 Hz, 2H), 7.97 (s, 1H); ^{13}CNMR (100 MHz, DMSO): δ = 21.50, 50.69, 52.93, 55.38, 55.68, 114.50, 125.92, 127.88, 130.17, 130.43, 131.56, 135.59, 143.17, 143.96, 159.00, 168.09 ppm; FT-IR (KBr): 3138, 2954, 1763, 1602, 1508, 1455, 1342, 1218, 1155, 1091 cm^{-1}. **3e**: ^{1}HNMR (400 MHz, DMSO): δ = 1.24 (t, *J* = 8.0 Hz, 3H), 2.39 (s, 3H), 4.20 (q, *J* = 8.0 Hz, 2H), 4.38 (s, 2H), 4.39 (s, 2H), 5.36 (s, 2H), 6.27 (m, 1H), 6.3 (m, 1H), 7.37 (d, *J* = 8.0 Hz, 2H), 7.52 (m, 1H), 7.69 (d, *J* = 8.0 Hz, 2H), 7.93 (s, 1H); ^{13}CNMR (100 MHz, DMSO): δ =14.43, 21.46, 42.35, 43.60, 50.75, 61.95, 110.28, 110.93, 125.87, 127.52, 130.09, 136.81, 142.69, 143.50, 143.64, 149.50, 167.59 ppm; FT-IR (KBr): 3330, 2985, 1750, 1508, 1468, 1417, 1371, 1185 cm^{-1}. **3f**: ^{1}HNMR (400 MHz, DMSO): δ =1.21 (t, *J* = 8.0 Hz, 3H), 2.41 (s, 3H), 3.72 (s, 3H), 4.16 (q, *J* = 8.0 Hz, 2H), 4.87 (s, 2H), 5.34 (s, 2H), 6.83 (d, *J* = 8.0 Hz, 2H), 6.96 (d, *J* = 8.0 Hz, 2H), 7.40 (d, *J* = 8.0 Hz, 2H), 7.54 (d, *J* = 8.0 Hz, 2H), 7.96 (s, 1H); ^{13}CNMR (100 MHz, DMSO): δ = 14.38, 21.50, 46.71, 50.81, 55.68, 61.90, 114.50, 125.88, 127.88, 130.16, 130.41, 131.59, 135.65, 143.16, 143.94, 159.01, 167.55 ppm; FT-IR (KBr): 3287, 2951, 1755, 1599, 1441, 1337, 1156 cm^{-1}. **4**: ^{1}HNMR (400 MHz, DMSO): δ = 2.14 (s, 3H), 2.42 (s, 3H), 4.91 (s, 2H), 5.39 (s, 2H), 7.09 (d, *J* = 8.0 Hz, 2H), 7.30 (m, 3H), 7.39 (d, *J* = 8.0 Hz, 2H), 7.52 (d, *J* = 8.0 Hz, 2H),

7.81 (s, 1H); ^{13}CNMR (100 MHz, DMSO): δ = 21.51, 27.37, 46.42, 58.61, 125.85, 127.84, 128.22, 128.86, 129.34, 130.19, 135.53, 139.26, 142.88, 144.05, 201.22 ppm.

3. Results and discussion

N-propargylsulfonamides **1** are readily prepared from the commercial available materials. Reaction of *p*-toluenesulfonyl chloride with an amine in pyridine for two hours at room temperature gives the corresponding sulfonamide in excellent yield. Treatment of the synthesized sulfonamide with propargyl bromide in the presence of K_2CO_3 in CH_3CN at 80 °C affords the *N*-propargylsulfonamides **1**.

With the *N*-propargylsulfonamides **1** and α-haloester **2** in hand, we turned our attention to the CuAAC reaction. To find the optimal conditions, the reaction of ethyl 2-bromoacetate **2a**, sodium azide and *N*-propargylsulfonamide **1a** was used as a model reaction. A mixture of **2a** (1 mmol), sodium azide (1.2 mmol) and solvent (5 mL) was stirred at room temperature for 1 h and then *N*-propargylsulfonamide **1a** was added to the mixture and was stirred under various reaction conditions (Table 1). In the absence of catalyst the product was not produced even after 10 h (entry 1). Using organic solvents such as ethanol and methanol decrease the reaction yield. Sodium azide is not very soluble in organic solvents (entries 3 and 4). In the mixture of water/ethanol (1:1), the yield of the reaction increased to 68% (entry 5). The effect of temperature was also investigated by carrying out the model reaction at 80 °C. The yield of **3a** was not affected more as the reaction temperature was raised (entry 6). The model reaction was accomplished by using Sharpless catalytic system which moderate yield of the desired product **3a** was obtained (Table 1, entry 7). Thus, as shown in Table 1 heating of **1a** with **2a** and NaN_3 at 60 °C in the presence of CuI (10 mol%) in the mixture of ethanol/water (1:1) were determined as optimal reaction conditions which resulted the desired triazole derivative **3a** in good yield (75%).

Table 1. Optimization conditions of the model reaction for synthesis of **3a**.

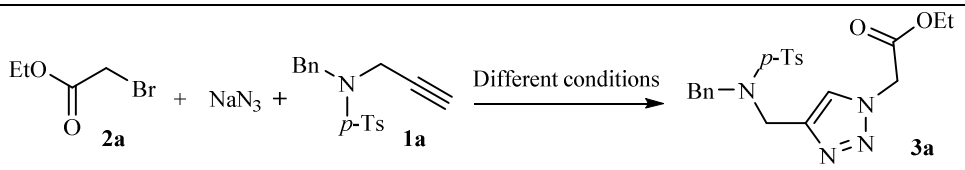

Entry	Catalyst	Solvent	Yield (%)[a]
1	-	H_2O/EtOH	-
2	CuI	H_2O	42
3	CuI	EtOH	39
4	CuI	MeOH	27
5	**CuI**	**H_2O/EtOH**	**75**
6	CuI [b]	H_2O/EtOH	67
7	$CuSO_4$/ sodium ascorbate (20 mol%)	H_2O/EtOH	51

[a] Reaction conditions: Solvent (5 mL, 1:1), *N*-propargylsulfonamide **1a** (1 mmol), ethyl 2-bromoacetate **2a** (1 mmol), NaN_3 (1.2 mmol), catalyst (10 mol%), 60 °C and reaction time 10 h; [b] at 80 °C.

With the optimized conditions in hand, various *N*-propargylsulfonamides **1** were allowed to react with α-haloesters **2** and sodium azide in the presence of CuI in water/ethanol. All the substrates efficiently proceed to give the corresponding 1,2,3-triazole derivatives **3** in good yields (Scheme 3). The results of ^{1}H, ^{13}C NMR and FT-IR spectral data reflected the assigned structure of the synthesized products. As a representative example, ^{1}H NMR, ^{13}C NMR and FT-IR spectral data of the compound **3c** are discussed in following section (computation section) and compared with DFT calculated data.

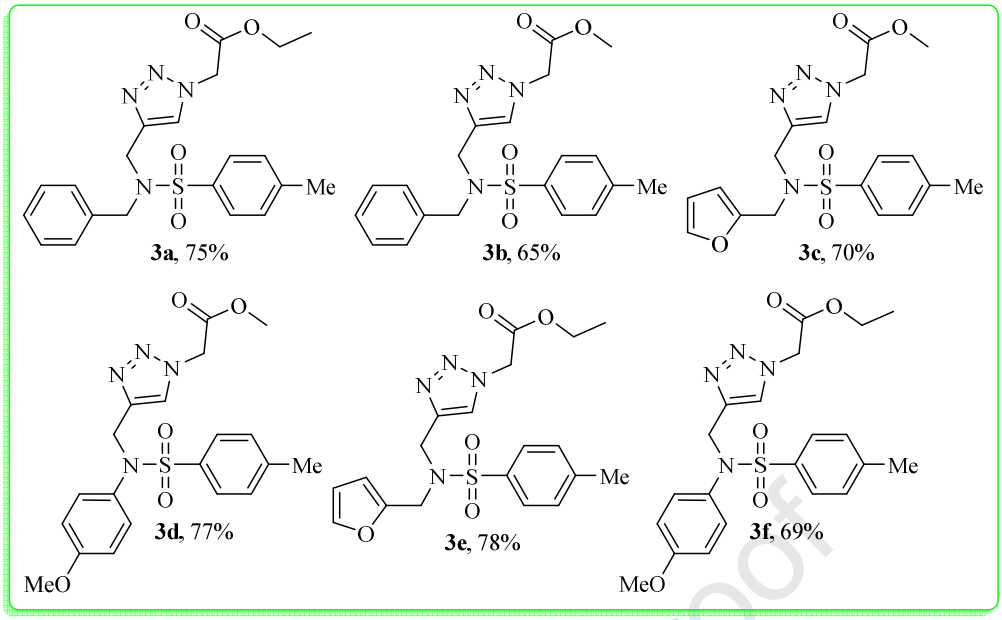

Scheme 3. The synthesis of novel 1-ester 4-sulfonamide-1,2,3-triazole derivatives **3**.

Interestingly, when 2-chloromethylacetoacetate was used as a substrate, the cycloaddition reaction takes place along with the decarboxylation of the 1,2,3-triazole product, leading to 1-acetyl 4-sulfonamide-1,2,3-triazole **4** (Scheme 4).

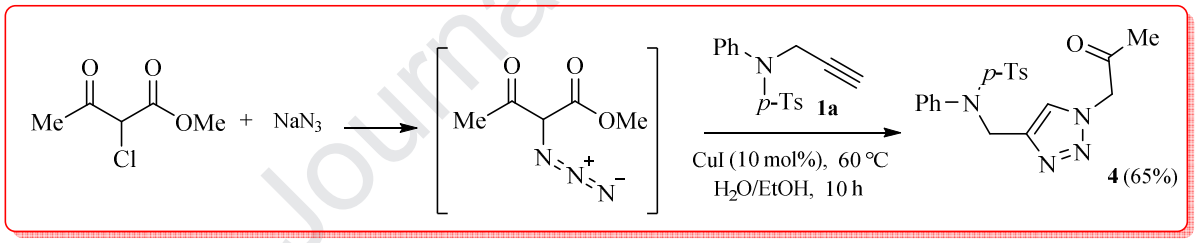

Scheme 4. Efficient synthesis of 1-acetyl 4-sulfonamide-1,2,3-triazole derivative **4**.

A plausible mechanism for the preparation of 1,2,3-tiazole derivatives **3** was suggested in Scheme 5. First, *N*-propargylsulfonamide interacts with CuI to form intermediate **A**, as a copper acetylide, followed by coordination of α-azidoester **B** to the copper of the acetylide initiates a thermally allowed [4πs + 2πs] cycloaddition reaction. Removal of copper from intermediate **C**, leads to the desired product **3**. It should be mentioned that formation of α-azidoester proceeds via a SN_2 mechanism. Direct substitution reaction of azide ion take place rapidly in α-azidoester or α-azidoamide systems. The π-LUMO of the carbonyl group in these substrates provide extended

conjugation, which can be stabilized the transition state in the S_{N2} mechanism [37], so α-haloesters compounds afforded the corresponding 1,2,3-triazoles in good yields, as shown in Scheme 3.

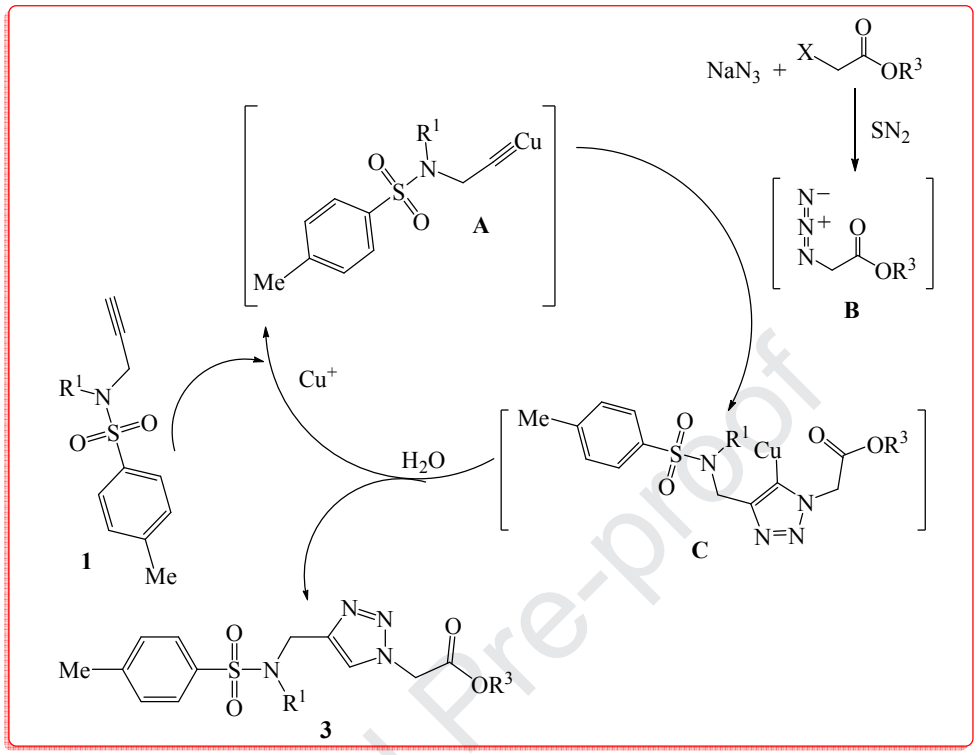

Scheme 5. Proposed mechanism for synthesis of 1,2,3-triazole derivatives **3**.

With the encouraging experimental data of 1-ester 4-sulfonamide-1,2,3-triazole derivatives **3**, our attention was turned on DFT calculations for investigation of physicochemical properties of **3c** such as electrophilicity index (HOMO-LUMO analysis), spectral data (FT-IR and NMR), and its interaction with Li^+ and Na^+. It should be noted that the computational methods have become a very useful and trustable tool for chemists. Moreover, DFT-B3LYP computational method is utilized by organic chemists as a straightforward and fast method for a variety of chemical calculations [38-47]. This method has been utilized here for performing the computations. Optimized structure for the B3LYP/6-31G(d) of **3c** is shown in Fig. 1. The obtained DFT data of **3c** is listed in the Table 2.

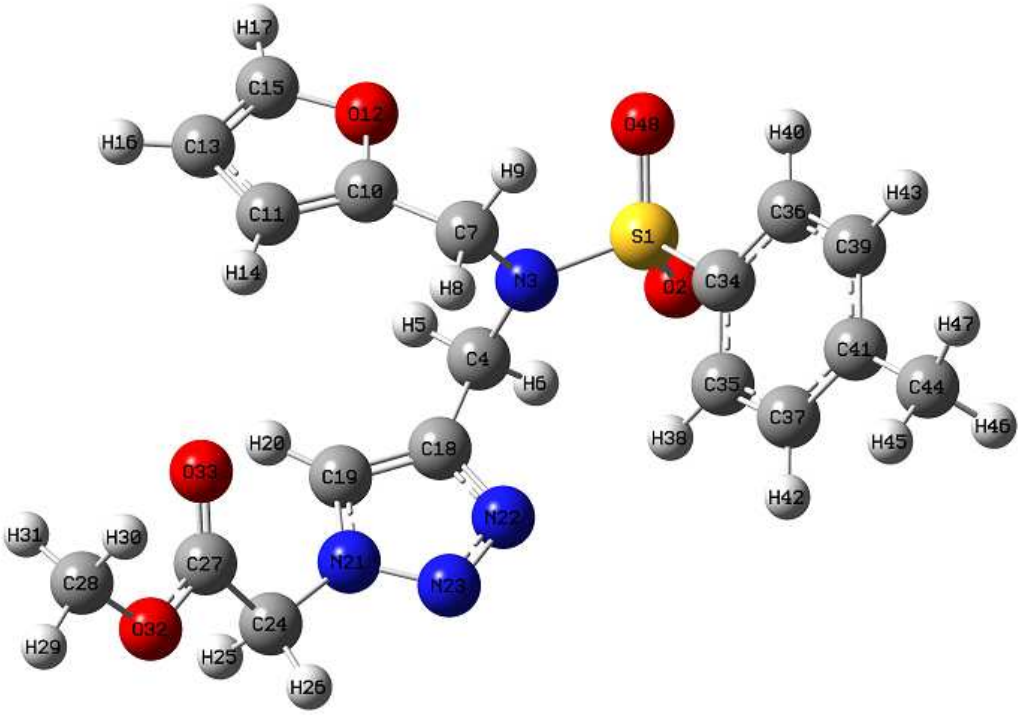

Fig. 1. Optimized geometry for the B3LYP/6-31G(d) of **3c**.

Table 2. The obtained DFT data of molecule **3c** at B3LYP/6-31G(d) level.

Parameter	Value
Energy (Hartree)	-1691.146
μ_D (Debye)	9.376
E_{HOMO} (eV)	-0.221
E_{LUMO} (eV)	-0.021
E_g (eV)	0.2
Chemical potential (μ) (eV)	-0.121
Chemical hardness (η) (eV)	0.1
Electrophilicity (ω) (eV)	0.073

Dipole moment (μ_D) for **3c** is 9.37 which demonstrates it has high dipolar properties. One reason for this dipolar value is the presence of polar functional motifs, carbonyl and sulfonamide, in its structure. E_{LUMO} is the energy of the lowest unoccupied molecular orbital and E_{HOMO} is the energy

of the highest occupied molecular orbital. The HOMO reveals the ability to donate an electron, while the LUMO reveals the ability to accept an electron. E_{HOMO} and E_{LUMO} of **3c** are -0.221 eV and -0.021 eV, respectively (Table 1). Fig. 2 shows the graphical sketches of HOMO and LUMO orbitals of the molecule **3c**.

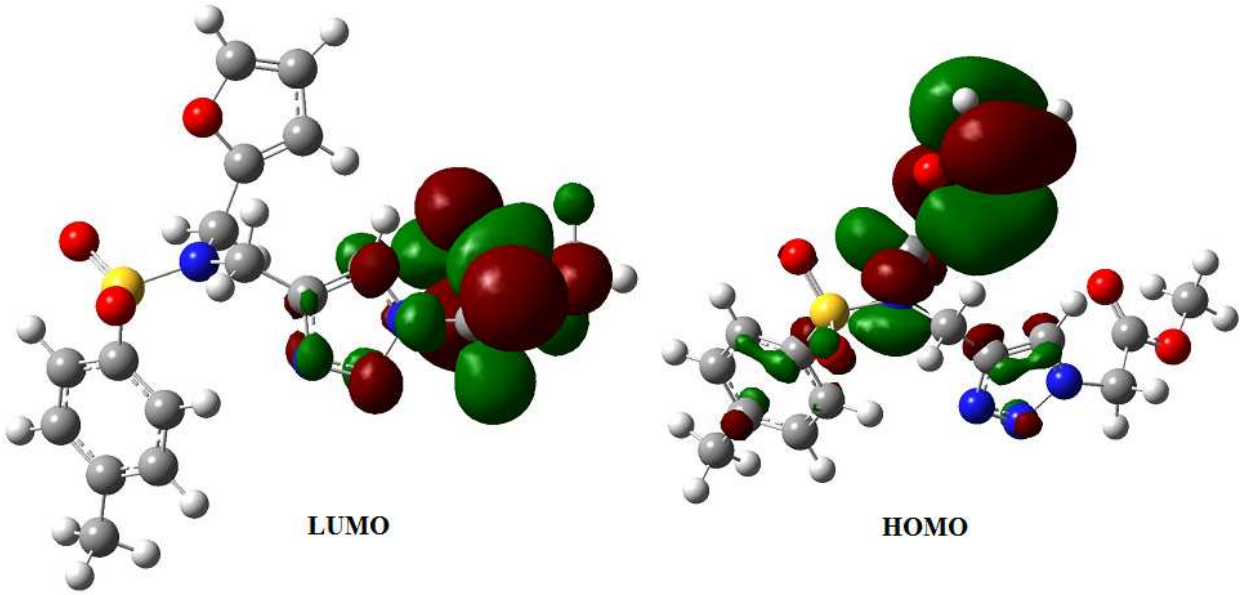

Fig. 2. Calculated HOMO and LUMO for **3c** at B3LYP/6-31G(d).

As shown in Fig. 2 the HOMO orbital is localized on furyl ring, while the LUMO orbital is mainly located on ester motif, due to bearing an electron withdrawing carbonyl group.

Electrophilicity is a fundamental object of organic compounds, which involves some adequate information regarding structure, reactivity, aromaticity, and toxicity, *etc*. [48-50]. Parr and coworkers defined electrophilicity (ω) as [51]:

$$\omega = \mu^2/2\eta \qquad (1)$$

$$\mu = (E_{LUMO} + E_{HOMO})/2 \quad \text{and} \quad \eta = (E_{LUMO} - E_{HOMO})/2 \qquad (2)$$

where μ and η are the chemical potential and chemical hardness, respectively given by equation (2). The electrophilicity index of **3c**, equals to 0.073 eV.

One of the main important goals of the DFT calculations is to properly assign the experimental frequencies to the computed vibrational modes of optimized structure of **3c**. The scaling factors 0.98 for below 1800 cm^{-1} and 0.99 for above 1800 cm^{-1} were applied for calculated frequencies

[52]. In general, there was a good agreement between experimental and calculated IR data. Triazole ring C-C stretching band for **3c** in simulated IR spectrum appears at 1597 cm^{-1}. The S=O stretching band for sulfonamide motif was appeared at 1304 cm^{-1} and its calculated counterpart appears at 1292 cm^{-1}. The characterized C=O stretching band for ester group were observed at 1751 cm^{-1}, while the corresponding calculated one appear at 1801 cm^{-1}.

The experimental ^{1}H NMR spectrum of **3c** consisted of two singlet signals at δ = 2.39 and 3.72 ppm for $-CH_3$ and $-OCH_3$ group, respectively, a multiplet signal at δ = 4.40 for two methylene groups ($-CH_2$), a sharp singlet peak at δ = 5.39 for the $–C\underline{H_2}CO$ group, two multiplet lines for furyl protons at δ = 6.27 and 7.36 ppm, five signals for furyl and phenyl protons at δ = 7.32–7.70 ppm, and one characteristic singlet peak for triazole proton at δ = 7.95 ppm. The ^{1}H–decoupled ^{13}C NMR spectrum of **3c** showed 16 resonances, which is in agreement with the proposed structure, with the ester carbon appearing at δ = 168.10 ppm, 10 distinct resonances for the aromatic carbons of phenyl, furyl and triazole groups between δ = 110.30-149.51 ppm, a peak at δ = 52.98 ppm for carbon of methoxy group, a line at δ = 50.66 ppm for $\underline{C}H_3CO$ and three distinct resonances at δ = 21.44-43.66 ppm for carbon of methylenes.

Representative B3LYP computed ^{1}H and ^{13}C chemical shifts for **3c** with experimental data are inserted in Table 3. It should be mentioned that the NMR calculations were done by using the gauge-independent atomic orbital (GIAO) method [53]. It should be mentioned that NMR calculations are sensitive for polarization function. The 6-31G(d) basis set is too small and cannot provide reliable results. Therefore 6-31+G(d, p) basis set was used for NMR calculations. On the other hand, since the experimental NMR spectra have been carried out in DMSO as solvent, the data of NMR chemical shifts for 6-31+G(d, p) optimized geometry **5c** in DMSO were also obtained in same basis set and solvent (Table 3).

Table 3. Representative 6-31+G(d, p) calculated and experimental ^{1}H and ^{13}C chemical shifts [a] of **3c**.

Atom[b]	$\delta_{exp.}$	$\delta_{6\text{-}31+(d,p)\ in\ the\ gas}$	$\delta_{6\text{-}31+(d,p)\ in\ DMSO}$
H_{45}	2.39	2.37	2.26
H_{30}	3.72	3.91	3.85
H_{25}	5.39	4.65	4.86
H_{20}	7.94	7.40	7.68
H_{5}	5.39	4.60	4.51
H_{8}	4.40	3.96	4.24
C_{44}	21.44	22.63	23.14
C_{24}	50.66	51.50	52.86
C_{28}	52.98	53.67	55.27
C_{27}	168.10	165.59	167.95
C_{11}	110.94	108.51	110.42
C_{13}	110.30	107.03	108.68

[a] In ppm; [b] For numbering of atoms refer Fig. 1.

The correlations of ^{1}H and ^{13}C NMR data in DMSO for 6-31+(d, p) basis set are presented in Fig. 3. The correlation coefficients for the ^{1}H and ^{13}CNMR data in the gas phase for 6-31+G(d, p) are also available in supporting information. The calculated ^{1}H and ^{13}C chemical shifts are in good agreement with the experimental data (Fig. 3).

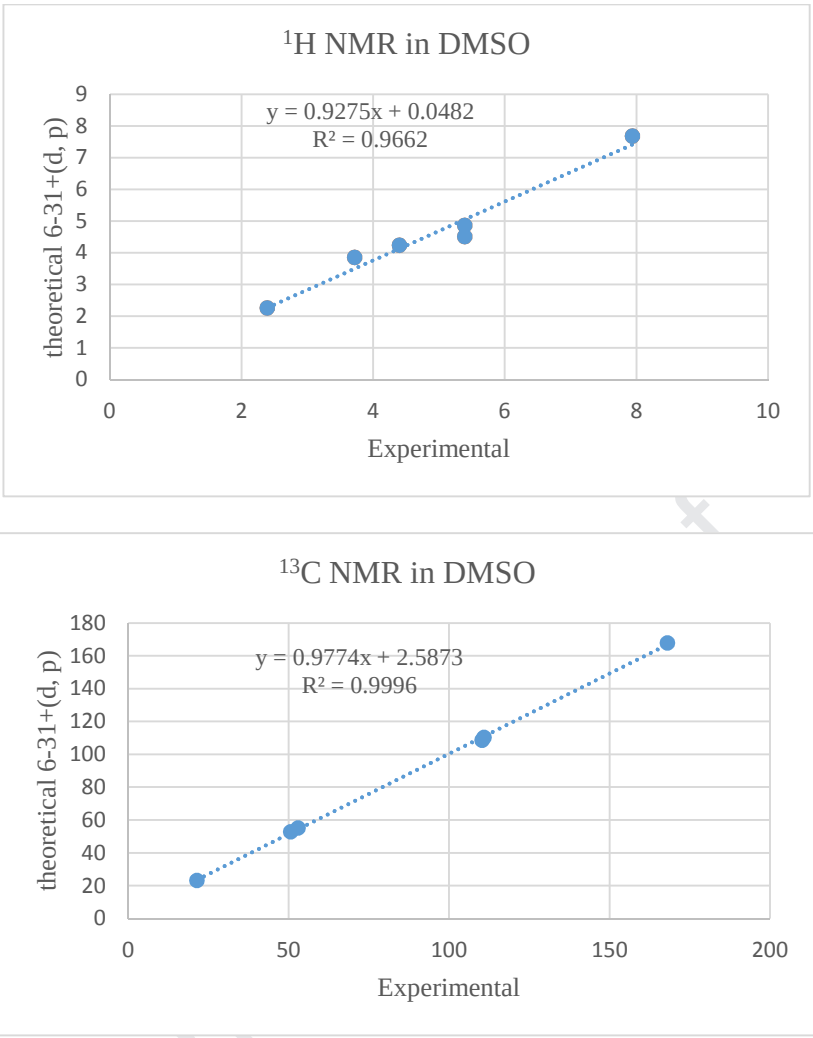

Fig. 3. The linear regression between experimental and 6-31+G(d, p) calculated ^{1}H and ^{13}C NMR data for **3c**.

It should be mentioned that chemical shifts were reported in parts per million relative to tetramethylsilane (TMS) for ^{1}H and ^{13}C NMR spectra. Relative chemical shifts were calculated by using the corresponding TMS shielding calculated at the same theoretical level and conditions as the reference.

In most of biological processes such as the stabilization of biomolecular conformations, osmotic balance, and information transfer *via* ion pumps, metal ions have vital rules. Sodium cation is the most important electrolyte in biological systems [54, 55]. Understanding of Li^{+} and Na^{+} ion interactions with the synthesized compounds **3**, and to obtain some information about the intrinsic binding poses of these ions to **3c**, can be useful. Cation affinity (CA) of **3c** can be determined in

the gas phase as the negative value of the enthalpy variation (ΔH) in the following reaction (Scheme 6) by using equation (3) [56].

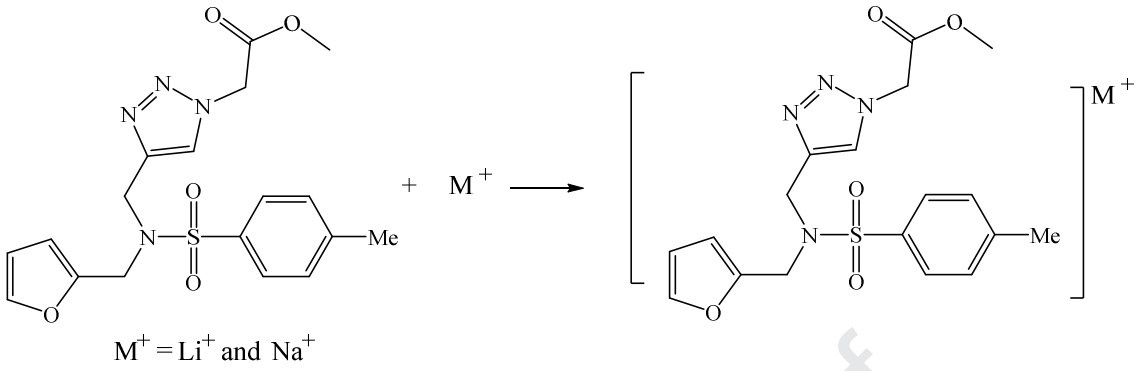

Scheme 6. Chemical process for cation affinity calculation of **3c**.

$$\mathrm{CA}(\mathbf{3c}) = -\Delta H = -\Delta E - \Delta(pv) = -\mathrm{E}(\mathbf{3c}\text{—}\mathrm{M}^{+}) + \mathrm{E}(\mathbf{3c}) + \mathrm{E}(\mathrm{M}^{+}) + \mathrm{RT} \qquad (3)$$

In equation (3) E is the total energy calculated for the optimized structures of both **3c** and metalated **3c** in the gas phase [57].

DFT calculations were done on structure of **3c**, metalated in its active sites. The cation can interact with **3c** at different positions: (**1**) with a nitrogen atom of triazole ring; (**2**) as a tetra-coordinated ligand with two nitrogen atoms of triazole ring, oxygen atom of furyl ring, and oxygen atom of O=C group, and (**3**) as a tri-coordinated ligand with oxygen atom of furyl ring, oxygen atom of O=S group, and nitrogen atom of sulfonamide motif. As shown in Fig. 4, the structure of **3c** is significantly changed during metalation.

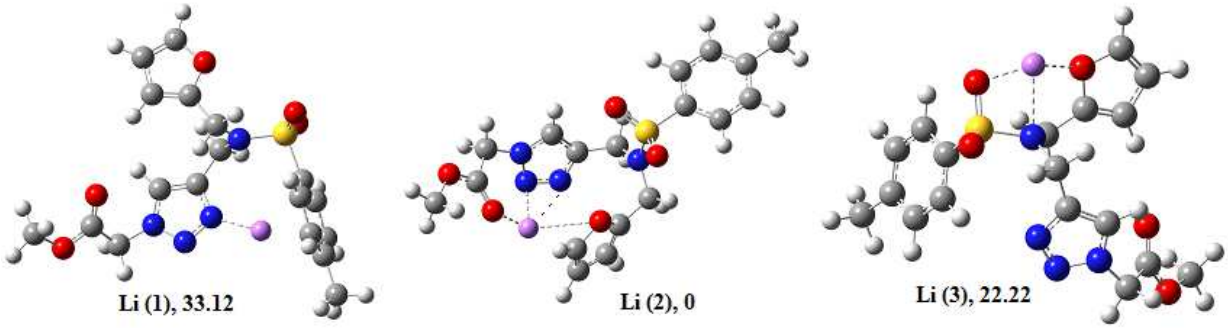

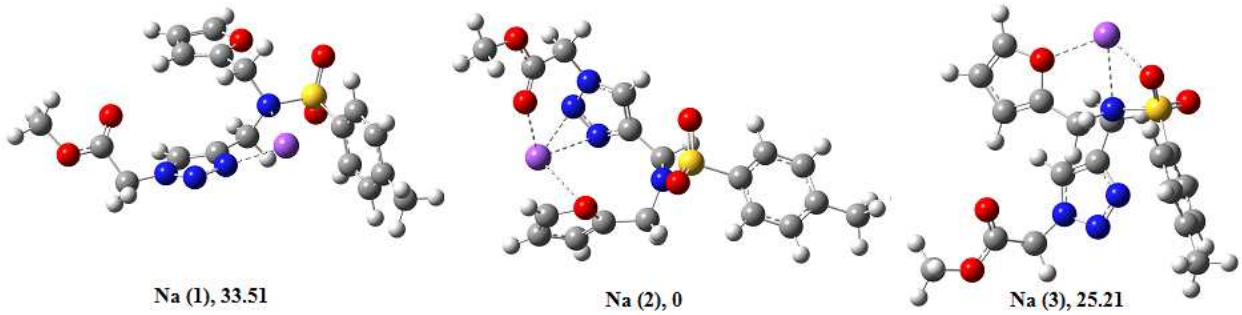

Fig. 4. Optimized structures of lithiated and sodiated **3c** at the B3LYP/6-31G(d) level and their relative energies in kJ/mol.

The tetra-coordinated complexes (**Li (2**) and **Na (2)**), are the most stable lithiated and sodiated structure of **3c**, in which M^+ has attractive electrostatic interaction with the nitrogen atoms of triazole group, oxygen atom of furyl ring, and O=C group (Fig. 4). DFT calculations show that the lithiation of **3c** is more exothermic than the sodiation. Difference in energies (80.78 kJ/mol) between **Li (2**) and **Na (2)** shows that in interaction of M^+ with the face a π system, Li^+ is in close proximity to aromatic rings in comparing of Na^+, due to its longer radius, positive charge is spread over large space than Li^+. Atomic charge in molecules has been used to describe the processes of electronegativity equalization and charge transfer in chemical reactions. Atomic polar tensor (APT) charges [58] affect electronic structure, dipole moment, and molecular polarizability. The ATP charge distribution structure of **Li(1)** and **Na(1)** are shown in Fig. 5. Most of the hydrogen atoms exhibit a net positive charge between 0.01-0.13 in APT analysis. All nitrogen atoms show negative charge in the range of -1.10 to -0.70. The Li and Na atoms in these complexes exhibit positive charge 0.602 and 0.762, respectively.

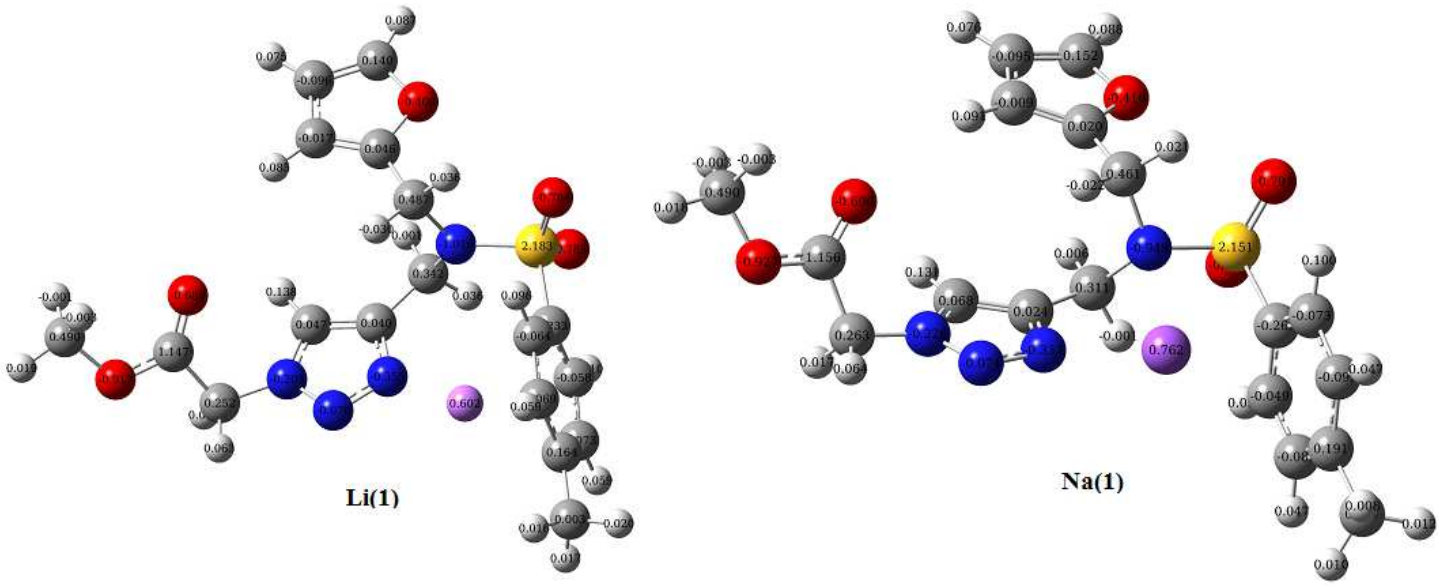

Fig. 5. The Atomic polar tensor charge distribution for **Li (1)** and **Na (1)**.

It is interesting to note that in complexes **Li (1**) and **Na (1)**, the cation can be interacted with π system of phenyl group (cation π interaction) [59, 60]. First evidence of this kind interaction in the gas phase was mentioned by Kebarle in 1981 [61]. The cation π interaction arises from the electrostatic interaction of M^+ with the face of a π system. Comparing of Na^+, Li^+ is in close proximity to aromatic rings, follows the classical electrostatic interaction (Fig. 4. In comparing with other structures of the complexes, **Li (1)** and **Na (1)** have not lowest energies. Heteroatom-cation interactions (the complexes **Li (2)**, **Li (3)**, **Na (2)** and **Na (3)**) are stronger that the cation π interaction (Fig. 4).

Comparison of aromaticity index of phenyl group in **3c**, after metalation with M^+, is also informative for cation π interaction. Aromaticity deals with the induced ring currents, therefore the magnetic susceptibility becomes more prominent for the aromaticity determination [62]. The nucleus–independent chemical shift (NICS) estimates the absolute magnetic shielding at the center of a ring [63, 64]. It should be noted that the more negative value of NICS, the more aromatic is the ring. It is expected that after metalation the aromaticity of phenyl group decreases. As shown in Fig. 6, in both lithiated **Li (1)** and sodiated **Na (1)** structures of **3c**, the aromaticity of phenyl

was decreased in comparing to unmetalated **3c** or complex **Li (2)**, in which Li^+ is coordinated with other sites of the molecule.

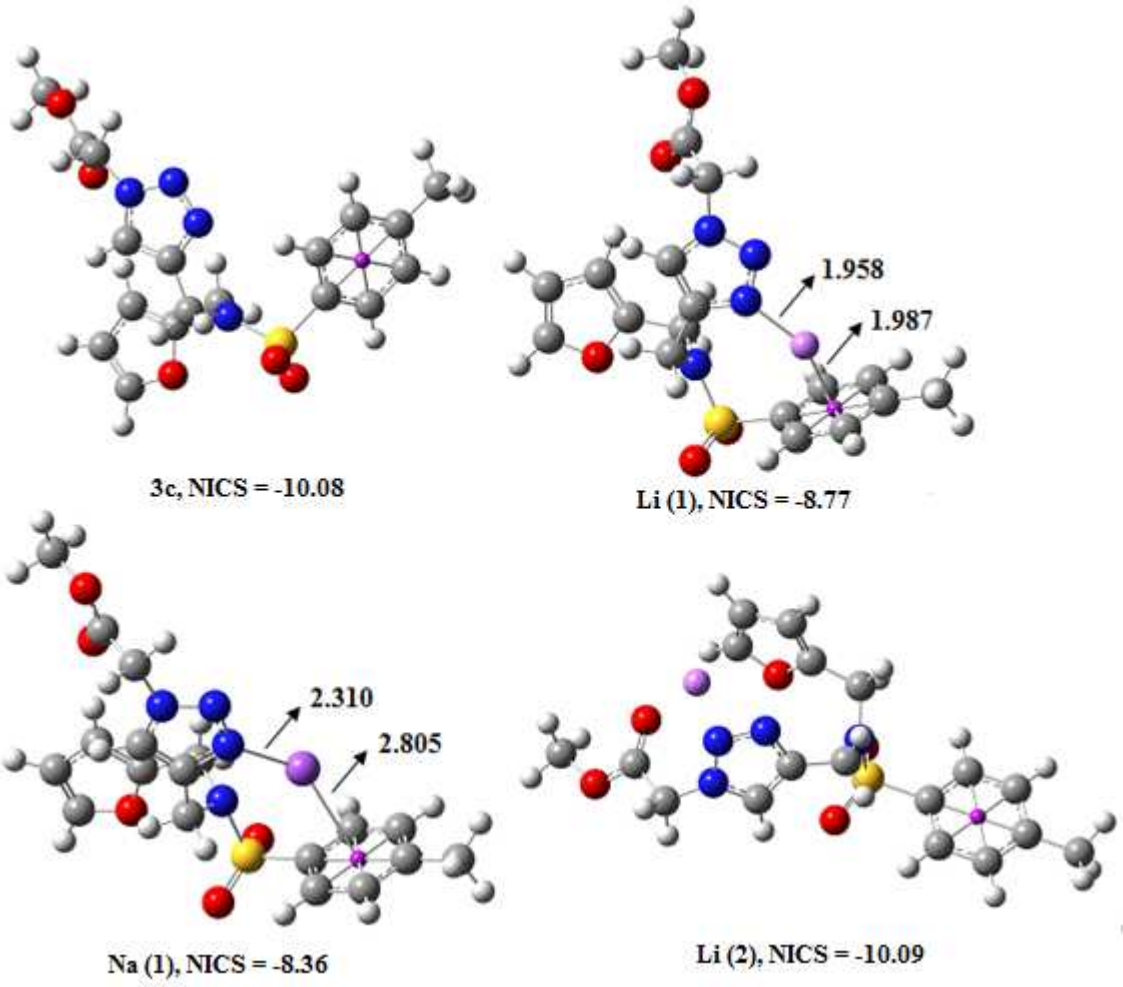

Fig. 6. The cation π interaction in complexes of **Li (1)** and **Na (1)** of **3c**. The bond distances are in Å. The NICS values are calculated at GIAO-B3LYP/6-31G(d) level and in ppm. The atom in center of phenyl group is a Bq atom as a probe.

It should be mentioned that the NICS values for phenyl group in **3c** and **Li (2)** are the same. The cation π interaction was also observed in furyl ring of complexes **Li (2)** and **Na (2)** of **3c** (Fig. 7).

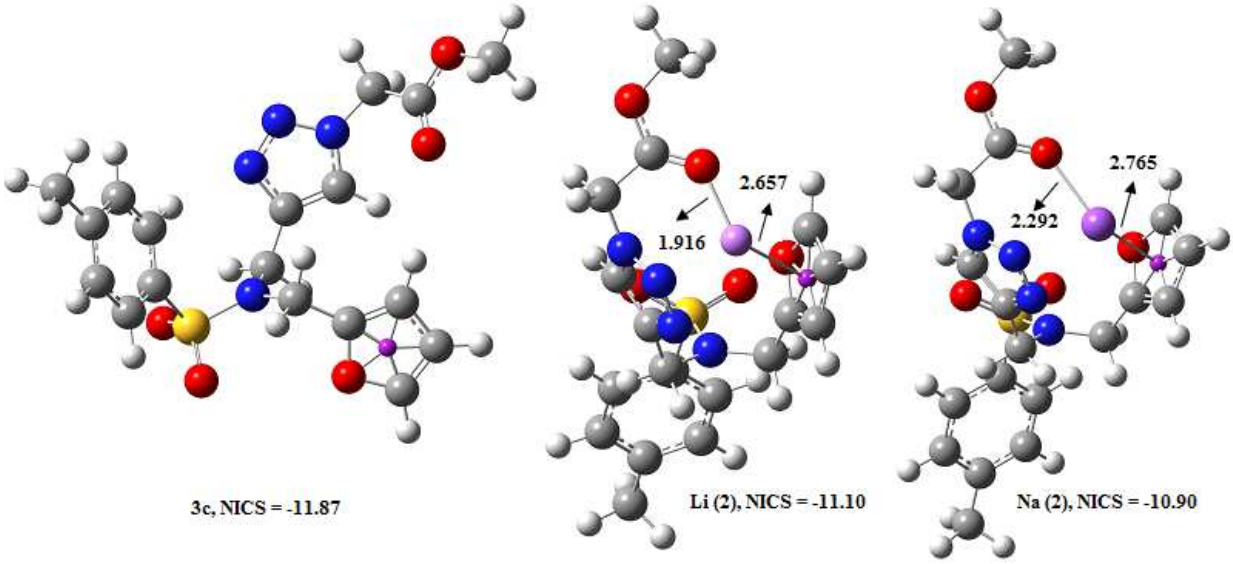

Fig. 7. The cation π interaction in complexes of **Li (2)** and **Na (2)** of **3c**. The bond distances are in Å. The NICS values are calculated at GIAO-B3LYP/6-31G(d) level and in ppm. The atom in center of furyl group is a Bq atom as a probe.

4. Conclusions

We have developed an efficient and practical protocol for the synthesis of 1-ester 4-sulfonamide-1,2,3-triazole derivatives as novel privileged scaffolds. The method is based on azidation of α-haloesters with sodium azide following by click azide–alkyne [3 + 2] cycloaddition reaction using H_2O/EtOH as a green reaction medium in the presence of 10 mol % of CuI. This click reaction takes place under mild and green conditions. Further work is in progress to synthesis of 1-ketone 4-sulfonamide-1,2,3-triazole derivatives. The HOMO-LUMO analysis, NMR and FT-IR studies of **3c** have been also studied using DFT calculations. The DFT results show that in some metalated structures of **3c**, there are some cation π interactions which for the first time, the NICS index was used to prove this kind of interaction.

Conflicts of interest

There are no conflicts to declare.

References

1. K. Lal, C. P. Kaushik, A. Kumar, *Med. Chem. Res*. **2015**, *24*, 3258-3271.

2. F. D. da Silva, M. C. B. V. de Souza, I. I. P. Frugulhetti, H. C. Castro, S. L .D. Souza, T. M. L. de Souza, D. Q. Rodrigues, A. M. T. Souza, P. A. Abreu, F. Passamani, R. F. Carlos, F. S. Vitor, *Eur. J. M. Chem*. **2009**, *44*, 373-383.

3. M. S. Costa, N. Boechat, E. A. Rangel, F. D. Da Silva, A. M. T. de Souza, C.R. Rodrigues, H. C. Castro, I. N. Junior, M. C. S. Lourenco, S. M. S. V. Wardell, V. F. Ferreira, *Bioorg. Med. Chem*. **2006**, *14*, 8644-8653.

4. M. J. Giffin, H. Heaslet, A. Brik, Y. C. Lin, G. Cauvi, C. H. Wong, D. E. McRee, J. H. Elder, C. D. Stout, B. E. Torbett, *J. Med. Chem*. **2008**, *51*, 6263–6270.

5. S. N. Darandale, N. A. Mulla, D. N. Pansare, J. N. Sangshetti, D. B. Shinde, *Eur. J. Med. Chem*. **2013**, *65*, 527-532.

6. S. Shafi, M. M. Alam, N. Mulakayala, C. Mulakayala, G. Vanaja, A. M. Kalle, R. Pallu, M. S. Alam, *Eur. J. Med. Chem*. **2012**, *49*, 324-333.

7. K. B. Sharpless, M. G. Finn, *Angew. Chem. Int. Ed.* **2001**, *40*, 2004-2021.

8. V. V. Rostovsev, L. G. Green, V. V. Fokin, K. B. Sharpless, Angew. 2002, **41**, 2596-2599.

9. C. W. Tornoe, C. Christensen, M. Meldal, *J. Org. Chem*. **2002**, *67*, 3057-3064.

10. M. Meldal, C. W. Tornøe, *Chem. Rev*. **2008**, *108*, 2952-3015.

11. R. Huisgen, *Angew. Chem.* **1963**, *75*, 604-606.

12. P. S. Rao, C. Kurumurthy, B. Veeraswamy, G. S. Kumar, P. S. Rao, R. Pamanji, J. V. Rao, B. Narsaiah. *Bioorg. Med. Chem. Lett*. **2013**, *23*, 1225–1227.

13. C. Proulx, W. D. Lubel, *J. Org. Chem*. **2010**, *75*, 5385–5387.

14. Z. Zheng, L. Shi, Tetrahedron Lett. **2016**, *57*, 5132–5134.

15. M. Saeedi, M. Safavi, E. K. Razkenari, M. Mahdavi, N. Edraki, F. H. Moghadam, M. Khanavi, T. Akbarzadeh. *Bioorg. Chem*. **2017**, *70*, 86–93.

16. F. Pagliai, T. Pirali, E. D. Grosso, R. Di Brisco, G. C. Tron, G. Sorba, A. A. Genazzani *J. Med. Chem.* **2006**, *49*, 467-470.

17. C. L. Su, C. L. Tseng, C. Ramesh, H. S. Liu, C. Y. F. Huang, C. F. Yao, *Eur. J. Med. Chem.* **2017**, *132*, 90-107.

18. W. Riemenschneider, H. M. Bolt, *Esters, Organic*, Ullmann's Encyclopedia of industrial chemistry, Wiley-VCH, Weinheim, **2005**.

19. J. M. Humphrey, A. R. Chamberlin, *Chem. Rev*. **1997**, *97*, 2243-2266.

20. M. Abdoli, A. Angeli, M. Bozdag, F Carta, A. Kakanejadifard, H. Saeidian, C. T. Supuran, *J. Enzyme Inhib. Med. Chem*. **2017**, *32*, 1071-1078.

21. X. L. Wang, K. Wan, C. H. Zhou, *Eur. J. Med. Chem*. **2010**, *45*, 4631-4639.

22. N. Pokhodylo, O. Shyyka, V. Matiychuk, *Med. Chem. Res*. **2014**, *23*, 2426–2438.

23. B. L. Wilkinson, L. F. Bornaghi, A. D. Wright, T. A. Houstonc, S. A. Poulsen, *Bioorg. Med. Chem. Lett*. **2007**, *17*, 1355-1357.

24. R. De Simone, M. G. Chini, I. Bruno, R. Riccio, D. Mueller, O. Werz, G. Bifulco, *J. Med. Chem.* **2011**, *54*, 1565–1575.

25. G. A. Sandip, R. M. Suleman, S. P. Vandana, *Chem. Asian J*. **2011**, *6*, 2696–2718.

26. V. Calderone, I. Giorgi, O. Livi, E. Martinotti, E. Mantuano, A. Martelli, A. Nardi, *Eur. J. Med. Chem.* **2005**, *40*, 521-528.

27. A. Brik, J. Alexandratos, Y. C. Lin, J. H. Elder, A. J. Olson, A. Wlodawer, D. S. Goodsell, C. H. Wong; *Chem. Bio. Chem.* **2005**, *6*, 1167-1169.

28. A. K. Jordao, P. P. Afonso, V. F. Ferreira, M. C. B. V. Souza, M. C. B. Almeida, C. O. Beltrame, D. P. Paiva, S. M. S. V. Wardell, J. L. Wardell, W. R. T. Tiekink, C. R. Damaso, A. C. Cunha, *Eur. J. Med. Ch*em. **2009**, *44*, 3777–3783.

29. M. V. Papadopoulou, W. D. Bloomer, H. S. Rosenzweig, E. Chatelain, M. Kaiser, S. R. Wilkinson, C. McKenzie, J. Ioset, *J. Med. Chem*. **2012**, *55*, 5554-5565.

30. H. Saeidian, S. V. Khajeh, Z. Mirjafary, B. Eftekhari, *RSC Adv*. 2018, **8**, 38801-38807.

31. Z. Mirjafary, L. Ahmadi, M. Moradi H. Saeidian, *RSC Adv*. **2015**, 5, 78038-78046.

32. H. Paghandeh, H. Saeidian, *J. Mol. Struct*. **2018**, *1157*, 560-566.

33. H. Saeidian, H. Sadighian, M. Abdoli, M. Sahandi, *J. Mol. Struct*. **2017**, *1131*, 73-78.

34. E. Taheri, Z. Mirjafary, H. Saeidian, *J. Mol. Struct*. **2018**, *1157*, 418-424.

35. H. Saeidian, H. Sadighian, M. Arabgari, Z. Mirjafary, S. E. Ayati, E. Najafi, F. M. Moghaddam, *Res. Chem. Intermed*. **2018**, *44*, 601–612.

36. J. M. Frisch, et al. Gaussian, Inc. Wallingford CT, Gaussian 09, Gaussian, Inc, **2013**.

37. F. A. Carey and R. J. Sundberg, *Advanced Organic Chemistry, Part A: structure and mechanisms*, Springer Science Business Media, LLC, Charlottesville, VA, 4th ed. **2007**.

38. H. Saeidian, M. Sahandi, *J. Mol. Struct.* **2015**, *1100*, 486-495.

39. B. Shams, H. Saeidian, *Comput. Theor. Chem*. **2018**, *1135*, 48-55.

40. A. Singh, A. K. Ojha, H. M. Jang, *ChemistrySelect* **2018**, *3*, 837-842.

41. M. Ghiasi, A. A. Oskouie, H. Saeidian, *Carbohyd. Res.* **2012**, *348*, 47-54.

42. A. J. Cohen, P. Mori-Sánchez, W. Yang, *Chem. Rev*. **2012**, *112*, 289-320.

43. P. Geerlings, F. De Proft, W. Langenaeker, *Chem. Rev*. 2003, **103**, 1793-1874.

44. H. Saeidian, M. Babri, D. Ashrafi, M. Sarabadani, M. T, Naseri, *Anal. Bioanal. Chem*. **2013**, *405*, 6749-6759.

45. H. Saeidian, M. Babri, M. Abdoli, M. Sarabadani, D. Ashrafi, M. T. Naseri, *Rapid Commun. Mass Spectrom*. **2012**, *26*, 2805-2814.

46. S. M. Patel, K. Pal, P. N. Kumar, M. Deepa, D. S. Sharada, *ChemistrySelect* **2018**, *3*, 1623-1628.

47. H. Saeidian, E. Barfinezad, *ChemistrySelect* **2019**, *4*, 3088-3095.

48. L. R. Domingo, P. Pérezb, J. A. Sáezc, *RSC Adv*. **2013**, *3*, 1486-1494.

49. P. K. Chattaraj, S. Giria, *Annu. Rep. Prog. Chem. Sect. C: Phys. Chem.* **2009**, *105*, 13-39.

50. P. K. Chattaraj, U. Sarkar, D. R. Roy, *Chem. Rev*. **2006**, *106*, 6, 2065-2091.

51. R. G. Parr, L. von Szentpaly, S. Liu, *J. Am. Chem. Soc*. **1999**, *121*, 1922–1924.

52. A. P. Scott and L. Radom, *J. Phys. Chem*. **1996**, *100*, 16502

53. K. Wolinski, J. F. Hinton, P. Pulay, *J. Am. Chem. Soc*. **1990**, *112*, 8251–8260.

54. J. A. Cowan, Inorganic Biochemistry: An Introduction, 2th ed. Wiley-VCH, New York, **1997**.

55. W. Kaim, B. Schwederski, Bioinorganic Chemistry: Inorganic Elements in the Chemistry of Life: An Introduction and Guide, Wiley, New York, **1994**.

56. H. Saeidian, *Turkish Comp. Theo. Chem*. **2017**, *1*, 1-7.

57. M. S. Ahmadi, M. Shakourian-Fard, A. Fattahi, *Struct. Chem*. **2012**, *23*, 613-626.

58. P.J. Stephens , K.J. Jalkanen , R.W. Kawiecki, *J. Am. Chem. Soc*. **1990**, *112*, 6518-6529.

59. J. C. Ma, D. A. Dougherty, *Chem. Rev*. **1997**, *97*, 1303-1324.

60. K. M. Ng, N. L. Ma, C. W. Tsang, *Rapid Commun. Mass Spectrom*. **1998**, *12*, 1679-1684.

61. J. Sunner, K. Nishlzawa, P. Kebarle, *J. Phys. Chem.* **1981**, *85*, 1814-1817.

62. J. A. N. F. Gomes, R. B. Mallion, *Chem. Rev*. **2001**, *101*, 1349-1384.

63. P. R. Schleyer, C. Maerker, A. Dransfeld, H. Jiao, N. J. R. E. Hommes *J. Am. Chem. Soc*. **1996**, *118*, 6317-6318.

64. H. F. B, Shaidaei, C. S. Wannere, C. Corminboeuf, R. Puchta, P. R. Schleyer, *Org. Lett*. **2006**, *8*, 863-866

1. The novel 1,2,3-triazole scaffolds were synthesized by using a CuAAC reaction.
2. DFT calculations were used to obtain physicochemical properties of the product **3c**.
3. Lithium ion affinity of **3c** was determined as 80.78 kJ/mol higher than its sodium affinity.

Declaration of interests

☒ The authors declare that they have no known competing financial interests or personal relationships that could have appeared to influence the work reported in this paper.

☐The authors declare the following financial interests/personal relationships which may be considered as potential competing interests: